Cu-Bound Formates are Main Reaction Intermediates during CO2 Hydrogenation to Methanol over Cu/ZrO2

F. Meunier, I. Dansette, A. Paredes-Nunez, Y. Schuurman

Cu-bound formates are main reaction intermediates during CO_2 hydrogenation to methanol over Cu/ZrO_2

Frederic C. Meunier*[a], Isaac Dansette[a], Anaelle Paredes-Nunez[a] and Yves Schuurman [a]

[a] Dr. F. C. Meunier, Dr. I. Dansette, Dr. A. Paredes-Nunez, Dr. Y. Schuurman,
Univ Lyon, Université Claude Bernard Lyon
CNRS, IRCELYON, 2 Av. Albert Einstein, 69626 Villeurbanne (France).
E-mail: fcm@ircelyon.univ-lyon1.fr

Supporting information for this article is given via a link at the end of the document

Abstract: Cu/ZrO_2 is a promising catalyst for the hydrogenation of CO_2 to methanol. Reaction pathways involving formates or hydroxycarbonyls have been proposed. We show here that three different types of formates can be observed under reaction conditions at 220 °C and 3 bar, one being located on metallic Cu and two others being bound to ZrO_2. The surface concentrations of formates were determined through calibration curves and their reactivity measured during chemical transient experiments. The Cu-bound formate represented only about 7 % of surface formates, but exhibited a higher reactivity and was found to be the only formate that could account for all the production of methanol. Copper is thus not there only to activate H_2, but also bears other crucial intermediates. This work reemphasizes that fully quantitative IR analyses and transient methods are required to unravel the role of surface species.

Introduction

There is a strong interest in developing technologies that can convert CO_2 into valuable chemicals, for instance, through hydrogenation with H_2 derived from renewable or nuclear energy. The hydrogenation of CO_2 to methanol (Eqn. 1) enables converting a waste greenhouse gas into a valuable fuel and chemical building block[1].

$$CO_2 + 3\ H_2 \Rightarrow CH_3OH + H_2O \quad \text{(Eqn. 1)}$$

$Cu/ZnO/Al_2O_3$ is the industrial reference when feeding CO-rich $CO/CO_2/H_2$ mixtures[2], but this catalyst suffers long term deactivation [3] that is expected to get worse under CO_2/H_2 mixtures, because of increased water concentrations favoring sintering[4,5]. Zirconia is highly stable hydrothermally[6] and has been used with Cu[1,7,8,9], Pd[10] or in metal-free mixed oxides[11] for the hydrogenation of CO_2 to methanol. Cu/ZrO_2 is a promising catalyst exhibiting high intrinsic activity[1], in which zirconia acts both as a support to disperse Cu and as an active component leading to a synergy with the metal[12,13].

The reaction mechanism taking place on Cu/ZrO_2 is still a matter of debate, hampering catalyst development. Reaction pathways involving formates have been often proposed[9, 14 , 15] . Yet, others have rejected formates as reaction intermediates and proposed the formation of CO through the reverse water-gas shift as a crucial step, followed by the formation of formaldehyde [16] or hydroxycarbonyls[17].

While the crucial role of formates appears to be put forward by the majority of groups, the location of those is unclear. Wu et al.[14] proposed that the reactive formates were located on the Cu metal. This conclusion echoes the seminal work of Waugh and co-workers who had proposed that Cu-born formates were the precursor to methanol[18,]. In contrast, other authors proposed that the reacting formates were located on zirconia[12,19], or more specifically at the Cu and zirconia interface[9,20].

We recently reported that at least two types of formates were present on the ZrO_2 phase on a 6 wt.% Cu/ZrO_2 catalyst and that the reactivity of those greatly differed[21]. The fastest reacting formates, which exhibited a 65-fold higher decomposition rate at 220 °C, was proposed to be located closer to the Cu-ZrO_2 interface.

In spite of the large numbers of IR studies existing on Cu-based catalysts for CO_2 hydrogenation, none to our knowledge has compared the specific rates of formate decomposition to that of methanol formation. We report here such comparison obtained through quantitative *operando* diffuse reflectance FT-IR spectroscopy (DRIFTS) on our Cu/ZrO_2[21]. Specific formate decomposition rates (in nmol s^{-1} g^{-1}) are derived from formate concentrations and decomposition rate constants.

The decomposition rates of the two ZrO_2-bound formates reported earlier[21] are significantly lower than that of methanol formation. Detailed IR signal analyses allowed to evidence highly reactive formates located on the Cu phase, the decomposition rate of which matched that of methanol formation. This study emphasises the complexity of the nature of adsorbates on a relatively simple catalyst formulation and the need to estimate quantitatively their reactivity.

Results and Discussion

The Cu/ZrO_2 catalyst was characterized in detail elsewhere [21] and the main findings are briefly recalled in the Supplementary Information section, including Cu dispersion, BET surface area and X-ray diffraction patterns (Figure S1).

The *operando* DRIFTS spectrum obtained at steady-state at 220°C and 3 bar of 20% CO_2 + 60% H_2 in He is shown in Figure 1A. As described earlier [21], IR bands of formates (2873, 1575 and 1380 cm^{-1}), carbonates (1468 cm^{-1}) and methoxides (2927, 2822, 1150 and 1049 cm^{-1}) were

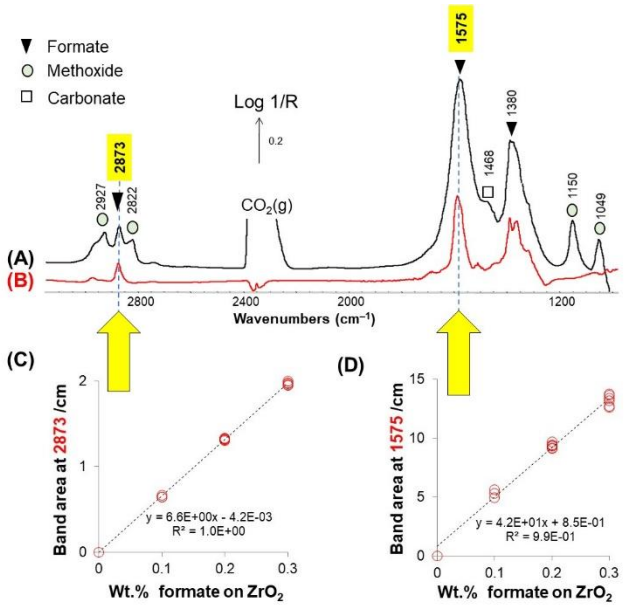

observed, located in most part on the zirconia support (Table 1). Most methoxides were likely spectators formed from the readsorption of methanol on ZrO_2, which are removed by hydrolysis with water rather than by reductive elimination, as shown by Fisher and Bell[12].

Figure 1. (A) DRIFTS spectra collected at steady-state at 220 °C over 6 wt.% Cu/ZrO_2 during the hydrogenation of CO_2 to methanol. Feed composition: 20% CO_2 + 60% H_2 in He, 3 bars total pressure. The spectrum of the reduced sample under H_2 taken just before CO_2 introduction was used as background (B) DRIFTS spectrum of the calibration standard 0.3 wt.% of formate on ZrO_2. The sample was held at 100 °C under He. The spectrum of bare ZrO_2 was used as background. (C) Calibration curve of ZrO_2-bound formates giving the area of the C-H stretching band at 2873 cm^{-1} versus formate loading (D) Calibration curve of ZrO_2-bound formates giving the area of the asymmetric O-C-O stretching band at 1575 cm^{-1} versus formate loading.

Table 1: Assignment of the main IR bands observed

Species	Wavenumbers (cm^{-1})	References
Formates on ZrO_2	2873, 1575, 1380	22, 23
Carbonates on ZrO_2	1468	12
Methoxy type I	2927, 2822, 1150	24,25
Methoxy type II	2927, 2822, 1049	24,25
Formates on Cu	2840, 1644, 1307	26

Formate calibration standards were prepared by dry-impregnating the support free of Cu with known amounts of a solution of sodium formate. Examples of DRIFTS spectra of the standard samples are given in Figure 1B and Figure S2. It is worth to stress that two separate formates bands could be used in the present case: one at 2873 cm^{-1} (C-H stretch) and another one at 1575 cm^{-1} (O-C-O asymmetric stretch). The similarity in wavenumber and band shapes between standards and spectra measured under reaction conditions, validates the use of this method. The precision of the standard measurements (each standard being measured at least three times, see Figure 1C and 1D) testifies of the

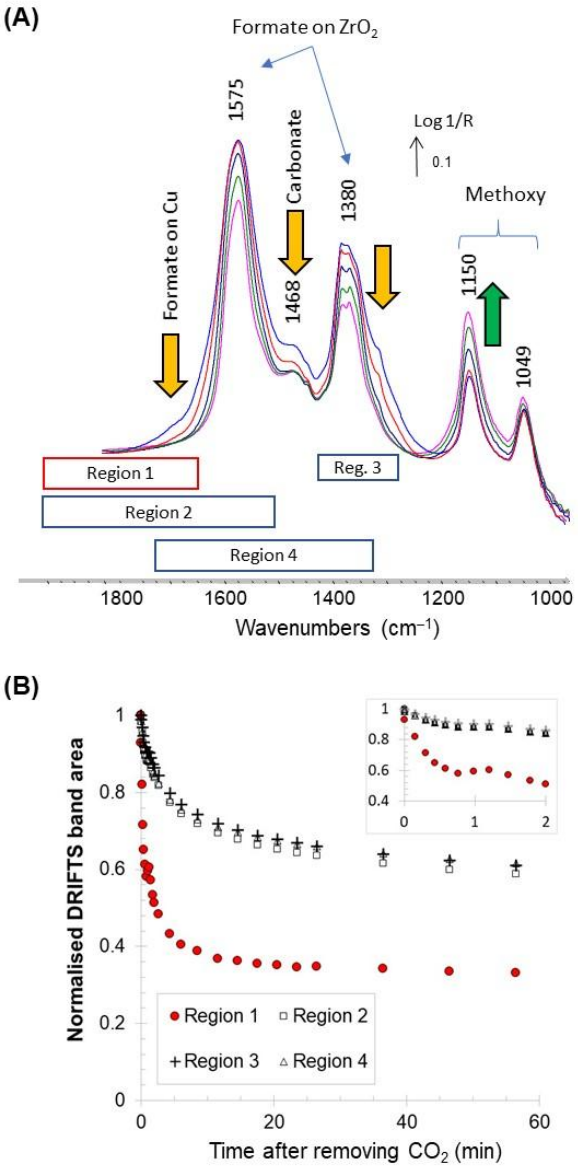

satisfactory reproducibility of the sampling method, i.e., loading the powder into the DRIFTS crucible. These calibration curves will be used to determine the concentration of each formate species observed under reaction conditions, the kinetic discrimination of which is now detailed.

Figure 2. (A) DRIFTS spectra collected over 6 wt.% Cu/ZrO_2 under 60% H_2 in He and 3 bars at various times following the removal of CO_2 from the feed. The first spectrum in blue is that at steady-state under CO_2 and H_2 shown in Figure 1A. The boxes underneath represent the four spectral intervals that were used to integrate the IR signal. (B) Corresponding normalized areas of the integrated four regions showing signal evolution over 60 min under H_2. The inset focuses on the first couple of minutes

The reactivity of formates present at the Cu/ZrO_2 surface was assessed by removing CO_2 from the feed (Figure 2). The IR signal evolution resulted from: (i) the reduction of part of the carbonates into formates and (ii) the hydrogenation of part of the formates into methoxy (Figure 2A).

Four regions were used to attempt to discriminate kinetically the various surface species reacting (see boxes in Figure 2A and Table S1). In our earlier work[21], only region 3

around 1380 cm^{-1} had been used, which mostly corresponds to ZrO_2-bound formates, as shown by Figure 1B. Signal integration using regions 2 (mostly associated with formates) and 4 (both formates and carbonates) led essentially to the same kinetic response as region 3 (Figure 2B, black symbols).

The fact that the same decay rate was obtained whether formates were integrated with carbonates or not indicates that carbonate signal contribution was minor and its effect could be neglected in these analyses. Most reports indicate that formate hydrogenation is the slowest reaction step and that carbonates are converted into formates during the process[19,27]. The carbonates observed were likely those located on ZrO_2 far away from the Cu interface and were thus only slowly reduced because of limited hydrogen spillover[12].

As discussed earlier[21], the decay observed using region 3 can be associated with so-called "fast formates", presumably located near the Cu interface and decaying within 25 min and "slow formates", presumably located far away from Cu and decaying much slower.

However, small yet significant changes also occurred on a timescale shorter than a minute, which were not addressed in our earlier study. The difference spectrum obtained 9 s after removing CO_2 from the feed showed a spectrum (Figure 3b, magnified 20 times) significantly different from that obtained at steady-state (mostly formates on ZrO_2, Figure 3a). The bands at 2840, 1639 and 1307 cm^{-1} are in fact fully consistent with a Cu-bound formate, as observed when adsorbing formic acid on Cu(100) [26].

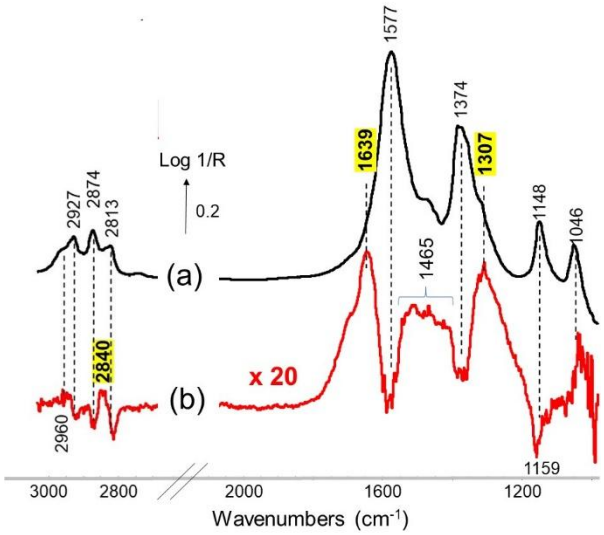

Figure 3. (a) DRIFTS spectrum collected over 6 wt.% Cu/ZrO_2 at steady-state under CO_2 and H_2 as shown in Figure 1A. (b) Difference spectrum between the steady-state signal and that collected 9 s after having removed the CO_2.

The ill-defined band at 1465 cm^{-1} indicated a loss of carbonates. Some "negative" bands (pointing downward) were also noted, related to species whose concentration had actually increased and corresponded exactly to ZrO_2-bound formates (1577 and 1374 cm^{-1}), presumably formed on the sites of lost carbonates. The negative band at 1159 cm^{-1} was related to newly formed methoxides, most likely on ZrO_2 and not on metallic Cu (the C-O stretch of methoxide on Cu(100) [28] is at 998 cm^{-1}).

The "negative" ZrO_2-bound formate and methoxide bands were corrected to obtain clear spectra of formates on Cu and these corrected spectra were used for quantification purposes (Figure S3A and S3B). The initial rate constant of decomposition of the Cu-bound formate was then derived using the signal obtained from the integration of region 1 (Figures 2 and S4 and Table S1), which gave the clearest corresponding IR signal. The signal was normalized over the first 0.4 min, yielding a linear decay with a rate constant noted "k" of 2.3 min^{-1} (Fig. 4A).

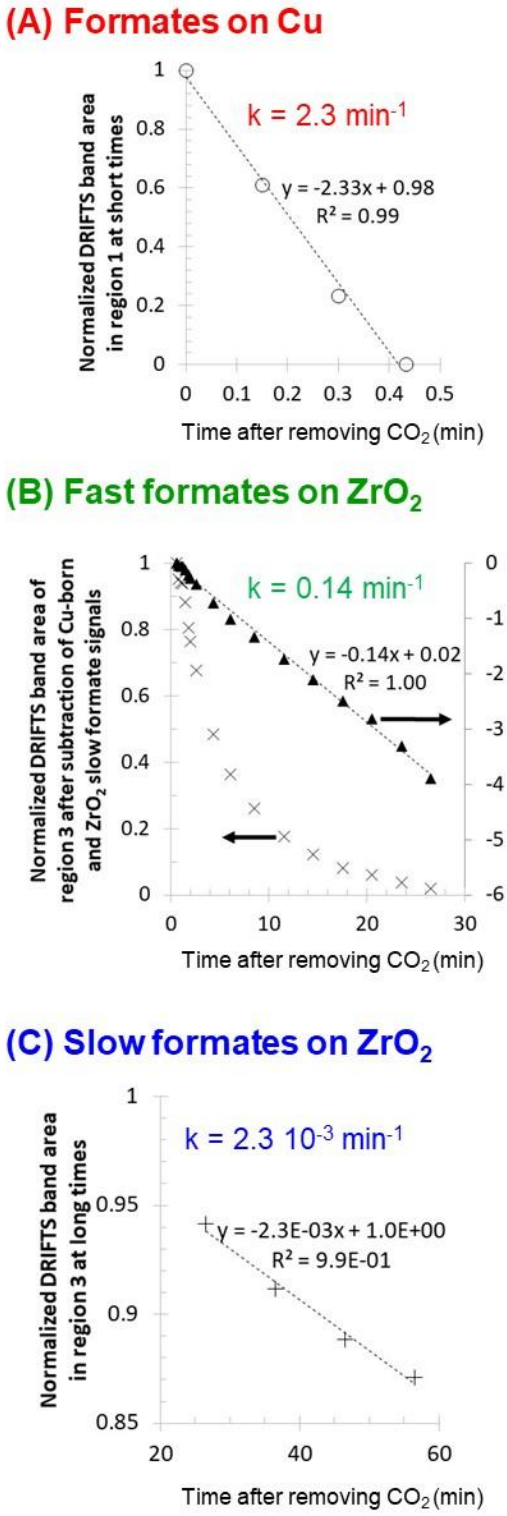

Figure 4. Normalized signal decay of (A) Cu-bound formates, (B) fast formates on ZrO_2 and the corresponding semi-logarithmic plot and (C) slow formates on ZrO_2. The corresponding initial rate constants of decay are also given.

The remaining signal after 0.8 min, which was free of any Cu-bound formates, was analysed using region 3, similarly to our previous study[21] (region 2, 3 and 4 yielding essentially the same response, as shown in Figure 2B). The decay of the slow formate on ZrO_2 from 25 to 60 min was essentially a straight line (Figure 4C) and assumed to follow the same trend from the origin of time.

The fast formate on ZrO_2 signal, after correction of the slow formate signal (see Ref. 21 for details), exhibited a single exponential decay over the 1 to 25 min period, indicating uniform reactivity (Figure 4B). This observation also stresses the relevance of the overall signal decomposition into these different contributions.

The initial rate constant of decomposition of the ZrO_2-bound species were about one and three-order of magnitude lower than that of the Cu-bound formates, respectively (Figure 4). The spectral differences obtained after these three critical periods are shown in Figure S5. The fast and slow formates on ZrO_2 exhibited essentially identical IR spectra, except for a slight shift of maximum band positions.

The specific rate of formate decomposition extrapolated at the time at which CO_2 was removed from the feed were calculated from (i) both formate calibration curves (Figure 1C and 1D) and (ii) the rate constants of decomposition (Figure 4). The IR calibration curves obtained from formates on ZrO_2 was used to determine formate concentration on Cu as an approximation. The derived formate concentration on Cu using calibration curve in Fig. 1C and 1D were 0.0945 and 0.133 wt.%, respectively. This is a reasonable agreement taking into account the difficulty of quantifying surface species. The calibration using the C-H stretching value (Fig. 1C) is likely to be the most accurate, since this bond is not directly interacting with the surface, unlike the formate carboxylate group. The averages of both values were used to reflect the error on the formate concentration measures.

Table 2. Decomposition rate constant k, concentrations and rates of decomposition of the various formates observed in the present study when CO_2 was removed from the feed at 220 °C and 3 bar, following steady-state under 20% CO + 60% H_2 in He. The rate of methanol formation at steady-state under the same conditions is also given. Calibration 1 and 2 refer to the curves in Figure 1C and 1D. The specific rates are given per mass of catalyst.

k(Cu-bound formates)	2.3	min^{-1}
k(ZrO_2-bound fast formates)	0.14	min^{-1}
k(ZrO_2-bound slow formates)	2.3×10^{-3}	min^{-1}
[Cu-bound formates], calibration 1 and 2 given in brackets	0.11 ± 0.025 (0.0945 ; 0.133)	wt.%
[Fast formates/ ZrO_2], calibration 1 and 2 given in brackets	0.44 ± 0.085 (0.380 ; 0.502)	wt.%
[Slow formates/ ZrO_2], calibration 1 and 2 given in brackets	0.95 ± 0.2 (0.817 ; 1.09)	wt.%
Cu-bound formate decomposition rate	**980 ± 200**	nmol s^{-1} g^{-1}
ZrO_2-bound fast formate decomposition rate	240 ± 50	nmol s^{-1} g^{-1}
ZrO_2-bound slow formate decomposition rate	8 ± 2	nmol s^{-1} g^{-1}
Rate of methanol production	**1010 ± 200**	nmol s^{-1} g^{-1}

Table 2 shows the formate concentrations calculated from the two different calibration curves, which led to a difference of ca. 20 %. The error on the rate constants was neglected in view of the prevailing one related to concentrations.

The specific rates of formate decomposition were simply calculated as the product of the corresponding k and concentrations and expressed in nmol s^{-1} g^{-1} (Table 2 and Figure 5). The Cu-bound formate exhibited a decomposition rate identical to that of methanol formation, within experimental error, and can thus be proposed as being a main reaction intermediate. In contrast, the ZrO_2-bound formates displayed decomposition rates significantly lower, indicating that those were not part of the main reaction pathway. In fact, the slow formate on zirconia, which contributed the most to the IR signal and displayed the largest loading on the sample, had a negligible contribution to methanol formation.

Using a zirconium atom surface concentration of 3.5 µmol m^{-2} [29], the coverage of ZrO_2 surface (ca. 115 m^2 g^{-1}) at steady-state by fast and slow formates were 25% and 53%, respectively. The rest were hydroxyls, methoxides and carbonates. The coverage of the Cu surface (ca. 8.3 m^2 g^{-1}) by fast formates was about 26%, assuming each formate coordinated to two copper surface atoms.

It should be emphasised that the relative contribution of the two main intermediates could vary significantly with pressure and other catalyst formulations (notably by altering the interface between Cu and zirconia), hence extrapolating these conclusions should be done with caution. Nonetheless, this work shows that detailed quantitative analyses and transient experiments should be carried out to discriminate main reaction intermediates and minor ones. These findings are summarized in Figure 6.

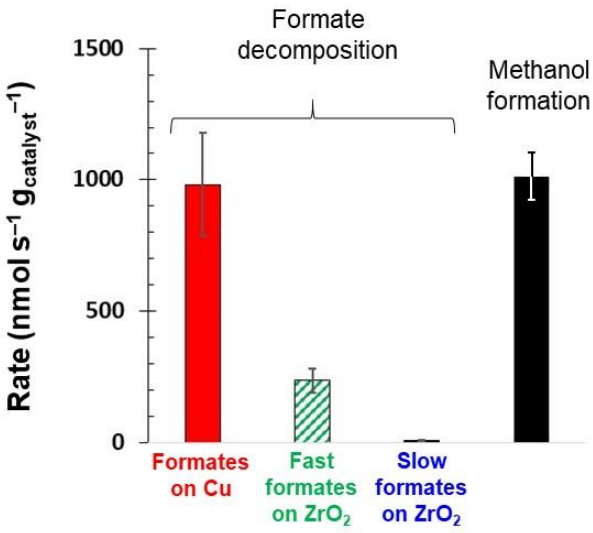

Figure 5. Specific initial reaction rates of formate decomposition for the three surface species observed and the rate of methanol formation at steady-state at 220 °C and 3 bar under 20% CO + 60% H_2 in He.

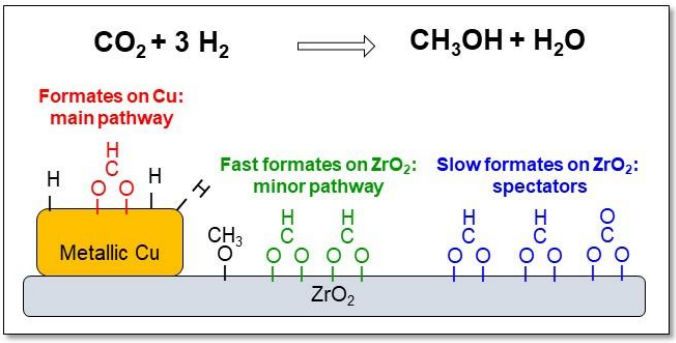

Figure 6. Schematic representation of the nature and relevance of surface species at the surface of a Cu/ZrO_2 catalyst used for CO_2 hydrogenation under 3 bar of 20% CO + 60% H_2 in He at 220°C.

Conclusion

In the present conditions, Cu-bound formates were identified as the main hydrogenation pathway to methanol, while zirconia-bound species were part of a minor pathway.

Acknowledgements

APN acknowledges a PhD grant from the University of Lyon.

Keywords: methanol • operando DRIFTS • structure-reactivity relationship • CO_2 hydrogenation • copper

[1] X. Jiang, X. Nie, X. Guo, C. Song, J.G. Chen, Chem. Rev. Chem. Rev. 2020, 120, 7984−8034.
[2] Kuld, S., Conradsen, C., Moses, P.G., Chorkendorff, I. and Sehested, J. (2014). Angew. Chem. Int. Ed., 53: 5941-5945.
[3] Golunski, S.; Burch, R. Top. Catal.**2021**, 64, 974–983.
[4] T. Lunkenbein, F. Girgsdies, T. Kandemir, N. Thomas, M. Behrens, R. Schlögl, E. Frei, *Angew. Chem. Int. Ed.* **2016**, *55*, 12708−12712.
[5] Pavliši˘c, P.A.; Ruiz–Zepeda, F.; Kova˘c, J.; Likozar, B. Ind. Eng. Chem. Res. **2019**, 58, 13021–13029.
[6] W. Zhang, Z. Wang, J. Huang, Y. Jiang, Energy & Fuels 2021, 35, 9209–9227.
[7] Yang, M., Yu, J., Zimina, A., Sarma, B. B., Pandit, L., Grunwaldt, J.-D., Zhang, L., Xu, H., Sun, J., *Angew. Chem. Int. Ed.* 2023, e202216803; *Angew. Chem.* **2023**, e202216803.
[8] Amenomiya, Y. Appl. Catal. **1987**, 30, 57–68.
[9] K. Larmier, W.-C. Liao, S. Tada, E. Lam, R. Verel, A. Bansode, A. Urakawa, A. Comas-Vives, C. Copéret, *Angew. Chem. Int. Ed.* **2017**, *56*, 2318–2323.
[10] Pinheiro Araújo, T., Mondelli, C., Agrachev, M. *et al.*. *Nat Commun* **13**, 5610 (2022).
[11] M.S. Frei, C. Mondelli, A. Cesarini, F. Krumeich, R. Hauert, J.A. Stewart, D. Curulla Ferré, J. Pérez-Ramírez, *ACS Catalysis* **2020** *10* (2), 1133–1145.
[12] Fisher, I.A.; Bell, A.T. J. Catal. **1997**, 172, 222–237.
[13] Li, K.; Chen, J.G. ACS Catal. **2019**, 9, 7840–7861.
[14] Wu, C., Lin, L., Liu, J. *et al.*. *Nat. Commun* **11**, 5767 (2020). https://doi.org/10.1038/s41467-020-19634-8
[15] L. Liu, X. Su, H. Zhang, N. Gao, F. Xue, Y. Ma, Z. Jiang, T. Fang, Appl. Surf. Sci. 2020, 528, 146900.
[16] J. Weigel, R.A. Koeppel, A. Baiker, A. Wokaun, Langmuir, 1996, 12, 5319–5329.
[17] Kattel, S.; Yan, B.; Yang, Y.; Chen, J.G.; Liu, P. J. Am. Chem. Soc. **2016**, 138, 12440–12450.
[18] G.J. Millar, C.H. Rochester, K.C. Waugh. Catal. Lett. 1992, 14, 289–295.
[19] Y.H. Wang, W.G. Gao, H. Wang, Y.E. Zheng, W. Na, K.Z. Li, RSC Adv., 2017, 7, 8709–8717.
[20] X. Chang, X. Han, Y. Pan, Z. Hao, J. Chen, M. Li, J. Lv, X. Ma, *Ind. Eng. Chem. Res.* **2022** *61* (20), 6872–6883.
[21] Meunier, F.C.; Dansette, I.; Eng, K.; Schuurman, Y. *Catalysts* **2022**, *12*, 793.
[22] Busca, G.; Lamotte, J.; Lavalley, J.C.; Lorenzelli, V. J. Am. Chem. Soc. **1987**, 109, 5197–5202. [
[23] Meunier, T.F.C.; Goguet, A.; Reid, D.; Burch, R.; Boaro, M.; Vicario, M.; Trovarelli, A. J. Catal. **2006**, 244, 183–191.
[24] Bensitel, M.; Moravek, V.; Lamotte, J.; Saur, O.; Lavalley, J.C. Spectrochim. Acta **1987**, 43, 1487–1491.
[25] Binet, C.; Daturi, M. Catal. Today, **2001**, 70, 155–167.
[26] B.A. Sexton, Surf. Sci. 1979, 88, 319–330.
[27] K.C. Waugh, Catal. Today, 1992, 15, 51–75.
[28] M. P. Andersson, P. Uvdal, A. D. MacKerell, *J. Phys. Chem. B* **2002** *106*, 5200–5211.
[29] K. Pokrovski, K.T. Jung, A.T. Bell, Langmuir, 2001, 17, 4297–4303.

Entry for the Table of Contents

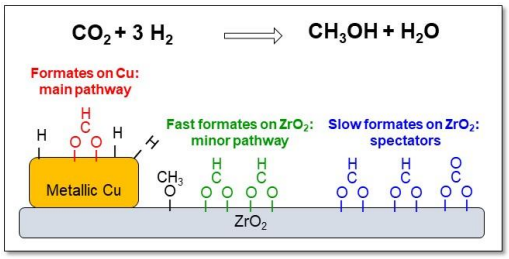

Cu-bound formates are the main reaction intermediates leading to methanol